ISSN: 2230-9926

Available online at http://www.journalijdr.com

IJDR

International Journal of Development Research
Vol. 10, Issue, 08, pp. 38714-38722, August, 2020
https://doi.org/10.37118/ijdr.19364.08.2020

RESEARCH ARTICLE OPEN ACCESS

PETROGRAPHIC, MINERALOGICAL AND GEOCHEMICALCHARACTERIZATION OF VOLCANIC PRODUCTS FROM NORTH-EAST MOROCCO

Hanane AIT HMEID[1*], Mustapha AKODAD[1], Mimoun AALAOUL[2], Mourad BAGHOUR[1], Abdelmajid MOUMEN[1], Ali SKALLI[1] and Lahcen DAOUDI[3]

1Laboratory Observatory of the Marchica Lagoon of Nador and Limiting Regions (OLMAN-RL), M ultidisciplinary Faculty of Nador, Moh amed 1st University, 60700 Nador –Morocco.
2Laboratory of Applied Geosciences, F aculty of Sciences of Oujda, Mohamed 1stuniversity, 60000 Oujda-Morocco
3Laboratory of Geosciences and Environment, Department of Geology, Faculty of Sciences and Technology, University Cadi Ayyad, Marrakech –Morocco

ARTICLE INFO

Article History:
Received 14th May 2020
Received in revised form
26th June 2020
Accepted 07th July 2020
Published online 26th August 2020

Key Words:

Bentonite, XRD, FTIR, XRF, microscopy, hydrothermal alteration, jbel Tidiennit, Morocco.

****Corresponding author:***
Hanane AIT HMEID

ABSTRACT

Seven types of bentonite pro files from the Trebia quarry located in the Jbel Tidiennit-Nador region (north-eastern Morocco) were sampled and studied for their physical, chemical, mineralogical and petrographic characteristics and evolution. Selected samples were analyzed by X-ray diffraction (XRD), IR spectroscopy (FTIR), chemical analysis (XRF) and the petrographic study (microscopy). The results show that clay minerals, K-feldspar, hematite, anorthite, and cristobalite were present as dominant phases with minor content of quartz, anatase, calcite, dolomite, xenotime, pyrite, rhodochrosite, and zeolite. A large amount of the main oxides in the Fe samples ranged between 28.6 and 48.9% Si content (from 0.1 to 16.7%). The clay fraction (<2 µm) consists mainly of smectite (> 90%), associated with trace amount of illite identified in all samples. In this study, we conclude of hydrothermal alteration.

Citation: ***Hanane AIT HMEID, Mustapha AKODAD, Mimoun AALAOUL, Mourad BAGHOUR, Abdelmajid MOUMEN, Ali SKALLI and Lahcen DAOUDI. 2020.*** "Petrographic, mineralogical and geochemicalcharacterization of volcanic products from North-East Morocco", *International Journal of Development Research*, 10, (08), 38714-38722.

INTRODUCTION

Bentonite generally refers to a clay minerals consisting essentially of montmorillonite mixed or interbedded with illite and/or kaolinite and other impurities (Inglethorpe et al.1993; Kouloughli 2007). They result from alteration and hydrothermal transformation of ash from glass rich volcanic tuffs originating from the neoformation of clay minerals, which are mainly part of the smectite group (Inglethorpe et al. 1993; Christidis et al. 1995).Bentonites have a wide range of industrial applications, such as refining and bleaching of glycerid oils clarification and purification of sugar solutions, syrups and wines water purification, sewage and effluent treatment pharmaceutical and therapeutic preparations absorbent (pet and animal litter oil spillage on factory floors). Catalytic action, carrier for catalysts Carrier for insecticides and fungicides mineral filler and extende , It is used in paste or powder form for the construction of waterp roof barriers for industrial and household waste (bentonite geomembranes) and radio- active waste (engineered barriers; compacted powder). In its liquid state, bentonite sludge is defined as a water-clay suspension. The origin of the use of sludge is undoubtedly oil drilling (Kelessidis et al. 2007), and Formulation of mortars, putties, adhesives, certain ceramic bodies. Demand for bentonite varies significantly from country to country. In the USA the largest producer, the major uses of bentonite have always been considered to be in bonding foundry sands, drilling fluids, and iron ore pelletising (Vista 1992). In Western Europe, the largest market for bentonite is currently pet litter. It is also used as a clarifying agent for oils and fats, in agriculture (as a carrier for pesticides and fertilizers and as a

coating for seeds), in civil engineering, in papexmaking, and in paints (Ross 1963; Grim and Guven 1978; Odom 1984). Bentonite deposits are located all over the world: the American continent (Canada, Brazil) (Knechtel and Patterson 1962), Africa (Morocco, Algiers, South African Union and Mozambique)(Termie r et al. 1956; Sadran et al. 1955). Europe and the eastern Mediterranean (Greece, Italy,...). In the western part of the American stat e of South Dakota and the eastern tip of Wyoming, locate the Black Hills region, the latter characterized by valuable bentonites for many industrial uses (Knechtel and Patte rson 1962). The Moroccan bentonite deposits are situated in northeastern side of Morocco (Frey et al. 1936; Azdimousa et al.2011). Due to the lack of studies of these bentonites deposit, our study focuses on the characterization of bentonite materials of the largest deposit from the Trebia, outcropping in the Tidiennit- Nador region associated with the Gourougou volcanic massif.

Geological setting From a geological point of view, the Trebia-Jbel Tidiennit deposit located in the Nador region belongs to the external domain of the Eastern Rifain chain (Louaya and Hamoumi 2010), which extends along the Mediterranean coast from the Nekor fault in the west to the mouth of the Moulouya River in the east (Maychou 2009) (Fig. 1).

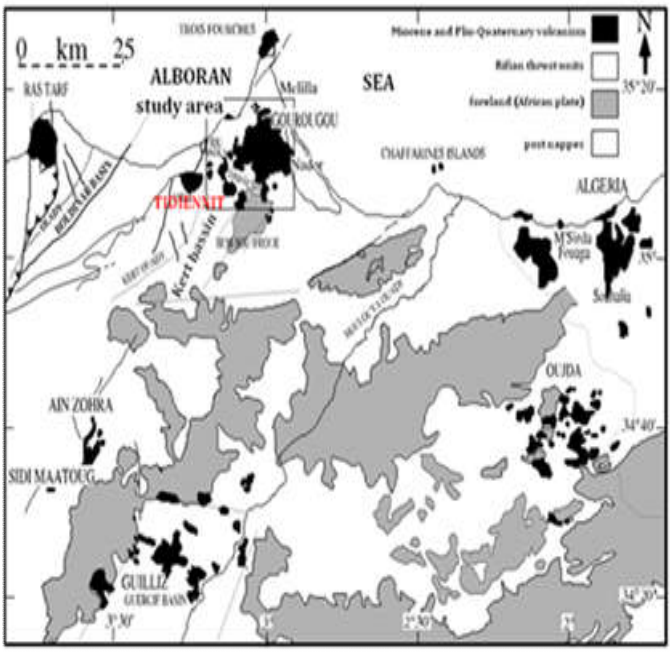

Fig. 1 Location of the study area (Geological map of the Rif belt (El Bakkali et al. 1998))

During their tectonic history, most of the sedimentary basins of the studied area were formed during the Messianian-Pliocene period, accompanied by subduction processes, inducing intense volcanic activity and formation of the Gourougou complex (Hernandez 1983; El Bakkali 1995; Ddani et al. 2005). During the formation of the neogenous basins, the lava, pyroclastic flows and ashes were deposited and then trans formed into bentonite deposits (Hernandez and Bellon 1985; El Bakkali et al. 1998; Ddani et al. 2005). Trebbia bentonites located in the northwestern flank of the Tidiennit massif (Fig. 2), bounded to the south by perlite and to the north by rhyolite, resulting in hydrothermal alteration of the lava dome (open system) (Ddani et al. 2005).

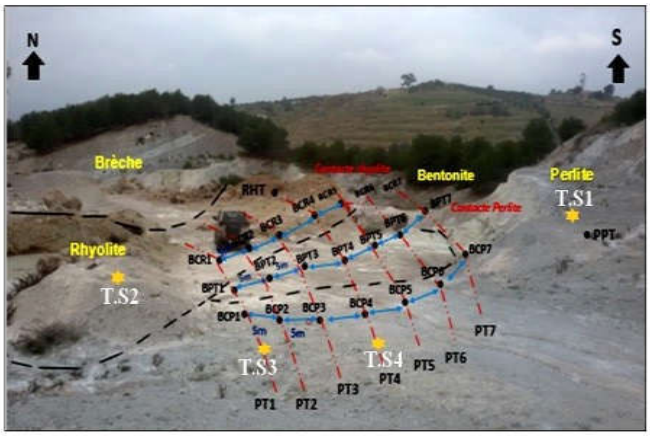

Legend: BPT_X: re al bentonite, BCP_X : contact bentonite with perlite, BCR_X : contact bentonite with rhyolite, TS_X : thin section.

Fig. 2 View of the Trebia-Jbel Tidiennit deposit and collected samples

MATERIALS AND METHODS

The sampling method consists of systematic collection in the form of a tight mesh with a pitch of 5 m (Fig. 2), at the level of the pure bentonites, also samples were taken at the level of perlite and rhyolite outcrops. The collected samples were dried in the oven at 60 °C for 48h and grounded with a mortar. Clay and non-clay materials were characterized by X-ray diffraction (XRD), infrared (FTIR), microscopy (thin section), particle size distribution, chemical analysis, and the measure of plasticity. The particle size distribution of the samples was analyzed on bulk sediment using a laser diffraction particle analyzer Horiba 300 (Department of Geology, Faculty of Sciences and Technology, Marrakech). The determination of the calcium carbonate content ($CaCO_3$) was determined using the Bernard calcimeter protocol according to the French standard NFP 94-048. Organic matter (OM) was determined by the method of loss on ignition (LOI) according to the protocol described by Heiri et al. (2001). The specific surface area was determined by adsorption of methylene blue. The test principle consists in determining the ionic adsorption capacity of clay particles, by measuring the amount of methylene blue dye necessary to cover the total surface, external and internal, under the conventional method, also called task test (Ngoc L an 1977). The measurement of free swelling index is carried out according to the French standard NF XP 84-703. Two grams of dried clay powder, crushed and passed through a 160-µm sieve, were poured into a graduated burette containing 100 ml of distilled water. After 24-48 hours, the total volume occupied by the clay was measured and water (Dixon et al. 1996). The mineralogy of the powdered bulk sediment and of the <2 µm fraction were determined using a Burker D8 diffractometer operating with CuKα radiations, according to the procedure for clay analysis described by Moore and Reynolds (1997). For the bulk sediment, analyses was given in a semi quantitative way (± 5 %) according to Cook et al. (1975). Intensity of the main diffraction peak of each mineral was measured and corrected by a multiplicative factor (Underwood et al. 2003). For the clay fraction, analyses were done according to normal procedure adopted by Moore and Reynolds (1989), clay fraction of each sample was decarbonated with HCl (0.1 mol. L^{-1}), the extraction of the clay fraction <2 µm from a suspension in water is based on the law of Stokes.

The three diagrams of X-ray were recorded sequentially as air dried or natural (N), after solvation with ethylene glycol for 24 h (EG) and heated at 500 ° C for 4 h ($H_{500C°}$). In order to study the surface characteristics of the bentonite and the identification of various forms of the minerals present in the clay, the infrared spectrophotometry with a Shimadzu FTIR-8400S IR spectrometer were carried out in the range 400- 4000 cm^{-1}. Liquid limit and plastic limit tests are obtained by determining Atterberg limits; the penetration test was carried out using the penetration cone method according to standards NF P-94-052-1(Laboratory of expertise, studies and tests, Marrakech, Morocco (ASTM D3418 1983). Chemical analysis of the samples (perlite, bentonite and rhyolite), was determined using an X-ray fluorescence analyzer.

RESULTS AND DISCUSSION

Particle size distribution: Tables 1 give the results of the grain size analysis of the bentonites raw material collected from Trebia deposits. The results show large particle size variations from one sample to another. For the analyzed Trebia materials, the clay fraction (<2 µm) has variable contents between 1.66 and 9.09%, the silty fraction varies between 20.81 and 92.79% and the sand fraction ranges between 1. 27 and 77.51%. The results of the granulometric analysis of the studied samples can be plotted in the McManus Ternary diagram (McManus 1988), following the relation between sand, silt and clay components and their controls on po rosity and permeability (Fig. 3). The diagram shows that, all the clay materials of Trebia are plotted in the area with moderately high porosity and permeability (Ait Hmeid et al. 2019).

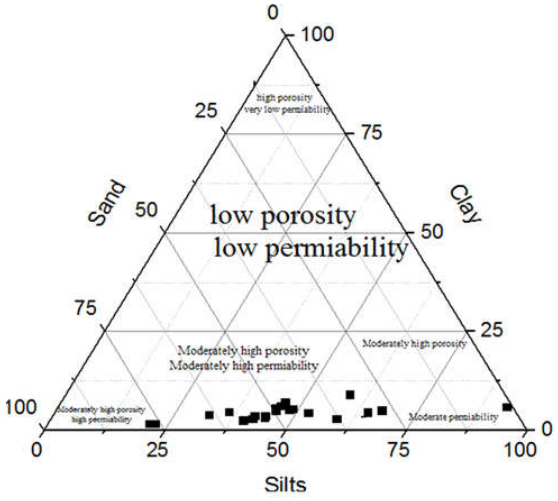

Fig. 3 Ternary diagram of studied bentonites following the relation between sand, silt, and clay com ponents and their controls over porosity and permeability. Af ter McManus 1988

Physicochemical parameters : Table 2 shows the different values of physico-chemical parameters related to our studied samples. The CaCO3 contents were very low (4-11%) except for BPT3 which was about 12% by weight and BPT5 of about 17%. The organic matter content values of all the samples are very low, it varies between 0.02% and 1.5%. Accordingly, a very low content of the total organic carbon was found in all samples; the percentage of TOC does not exceed 1.02%, and the total inorganic carbon (TIC) vary between 0.2% and 3.6%.

Table 1. Particle size distribution, of the studied samples in the Trebia deposit

Sample	% Sand (> 60 µm)	% Silts (2–60 µm)	% Clay (<2 µm)	LL %	PL %	PI %
BCP1	43.11	52.38	4.50	137	51	86
BCP2	1.27	92.79	5.93	74	34	40
BCP3	52.36	43.90	3.72	95	40	55
BCP4	77.51	20.81	1.66	102	42	60
BCP5	57.56	39.87	2.56	76	35	41
BCP6	59.44	35.92	4.63	113	45	68
BCP7	38.01	59.03	2.95	98	41	57
BCP8	27.60	67.32	5.07	89	39	50
BCR1	45.02	46.35	5.07	70	30	40
BCR2	46.56	46.27	7.16	89	37	52
BCR3	47.87	45.89	6.23	70	32	38
BCR4	49.22	45.05	5.72	84	37	47
BCR5	45.89	48.71	5.38	92	39	53
BCR6	32.20	58.69	9.09	89	40	49
BCR7	30.80	64.59	4.60	77	34	43
BPT1	63.91	32.12	3.95	90	38	52
BPT2	49.56	45.47	4.96	89	38	51
BPT3	55.35	41.66	2.98	94	40	54
BPT4	54.63	41.63	3.72	98	40	58
BPT5	76.17	22.08	1.74	88	38	50
BPT6	52.74	43.88	3.36	95	39	56

Trebia's materials have fairly high natural water contents which vary between 10.20 to 36.95%. These variations in natural water content may be related to the quantity of fine or clay elements contained in the samples analyzed. So we find that the humidity value is signi ficant in all the samples, which explains the hyg roscopic character and th e high value of the porosity (Rollet and Bouaziz 1972). The quantity of this water, in most cases, corresponds to that of the interlayer layers between the silicate sh eets, it is dependent on the nature of the ions adsorbed (Hyun et al. 2001).

Table 2. Physico-chemical parameters of the studied samples

Sample	Total MO content (wt.%)	TOC (wt.%)	TIC (wt.%)	water content (W %)	Total CaCO3 content (wt.%)	PH	SST ($m^2.g^{-1}$)
BPT1	1.40	0.51	1.90	28.73	11	9.12	518.92
BPT2	0.12	0.72	2.10	25.11	9	8.43	402.50
BPT3	0.10	0.97	2.10	24.55	12	7.75	358.39
BPT4	1.50	0.67	3.60	30.70	5	7.26	271.81
BPT5	0.12	0.76	0.80	30.91	17	6.87	314.73
BPT6	0.05	0.71	2.70	36.41	8	7.14	273.95
BCP1	0.13	0.61	2.70	16.28	11	9.23	351.17
BCP2	0.03	0.75	1.70	16.66	10	8.76	172.97
BCP3	0.14	0.88	1.70	16.69	5	8.03	310.84
BCP4	0.13	0.56	1.40	15.74	7	9.17	490.54
BCP5	0.12	0.52	1.90	15.79	7	8.97	693.04
BCP6	0.10	0.87	1.30	16.45	7	8.92	610.45
BCP7	0.16	1.02	2.20	16.23	7	8.45	365.90
BCP8	0.16	0.43	1.90	10.20	9	8.43	239.65
BCR1	0.08	0.51	2.70	30.63	7	6.94	160.17
BCR2	0.07	0.46	0.70	31.26	4	6.73	160.17
BCR3	0.16	0.57	0.80	28.41	6	6.66	160.17
BCR4	0.10	0.79	0.20	36.95	6	7.54	160.17
BCR5	0.08	0.83	1.90	19.66	7	7.25	160.17
BCR6	0.12	0.60	1.40	17.15	6	6.67	160.17
BCR7	0.02	0.67	0.65	21.20	8	6.90	160.17

The pH values vary from 6.66 to 9.23, this basicity would be due to the soluble and basic s alts such as the alkaline carbonates and bicarbonates or the silicates, and enter generally in the composition of the clay (Millogo 2008; Qlihaa

et al. 2016). The specific surface of bentonite from Trebia is characterized by a large specific surface area which varies between 127.62 m2 g-1 and 693.04 m2 g-1. This surface is likely to increase in aqueous solution according to the solid / liquid ratio which modulates the degree of hydration (Ait hmeid et al. 2020). The free swelling index of Trebia bentonites varies between 5 ml and 13 ml suggesting that the clay of Trebia has significant swelling properties, so to improve the quality of these bentonites, we have done the activation by soda and we have find values between 20 and 36%.

Fig. 4 Optical microscopic analysis of the thin section of the rhyolite sampleN.L (Natural light); P.L (Polarized light)

Petrographic study: Trebia rhyolite characterized by a light enough color, pink to yellowish colo r, with minerals visible to the naked eye: quartz, feldspars and biotite, in microlitic structure to the naked eye existence of la rge visible cryst als (phenocrysts) in a paste not crystallized (hemic ristalline structure) so it is a holohyaline rock .In thin section of the rhyolite (T .S_2) are shown in fig. 4, observe it big crystals and small crystals are microliths visible in a non-crystallized paste appearing black in polarized light analyzed it is a microlithic structure. The rhyolite has a glassy t exture like obsidian, but has radi al pseudo-crystals in the fo rm of radiated sph eres, which cover the surfaces of vol canic p anes called spherulites, which gives rhyolite a spherulitic texture. The main constituents are spherulites, partially plagioclase in the form of phenocrysts and som etimes twinned, Quartz, feldspar (Zonea) biotite and opaques consist mainly of titano-magnetite (possibly hematite, magnetite or ilmenite) (Abdelouas 1996), the presence of these minerals has been confirmed by X-ray analysis.

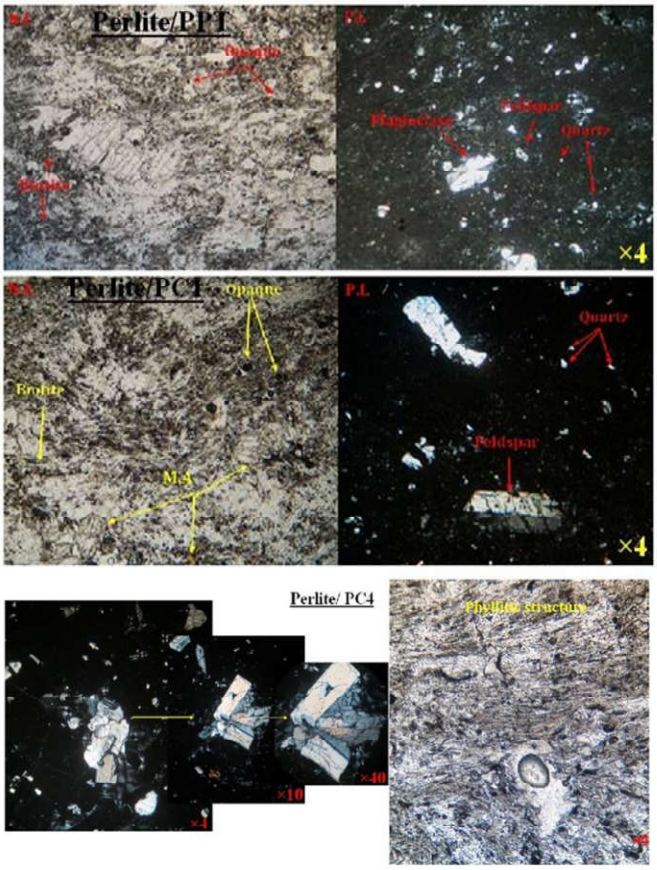

Fig. 5. Optical microscopic analysis of the thin section of the perlite samples

The glass matrix displays a pearlitic texture in which microlites have developed in pearlitic fractures perhaps the appearance of pearlite.In crystallized vitreous glass, with the presence of small crystals in the form of geodes they are microgeodes. The main perlite Trebia (T.S_1) (Fig. 5) has a fairly greyish to whitish color, in thin section we notice the presence of d ark gray fragm ents carpets on a fresh surface with the presence of a brown to gray surface it is the altered surface, mineralogically composed of phenocrysts of biotite, quartz, plagioclase, feldspar, and opaque, having a glassy texture contains globules separated by withdrawal slits gives the pearlitic texture. The passage at the contact with the bentonite (T.S_3) sample it is dark gray with black flow, constitute phenocrysts of feldspar strongly altered by fracture, biotite, quartz and opaque. The appearance of a yellow material may be due to alteration probably clays, zeolites or else o r a mineral of the silica group (Rotella and Simandl 1996). (T.S_4) showed phyllitic structure. In the literature,

Petrographically, perlite is defined as the hydration of natural rhyolitic glass with a pearlitic texture (Rotella and Simandl 1996), this explains the appearance the texture of the perlite at the level of the rhyolite, on the other hand the phyllite structure that appears at the level of the contact perlite it is the clay minerals (smectite), So the Trebia bentonites result from hydrothermal alterations from the perlite to the bentonites.

Mineralogical composition and geographic distribution

Bulk and clay mineralogy: Bentonites of Trebia are bordered to the south by perlite and to the north by rhyolite (Fig. 2), depending on their geographical position and mineralogical composition; three types of profiles can be distinguished. Figure 6.a and table 3 shows the untreated X-ray diffractograms of the total mine ralogy of bentonite, perlite and rhyolite. Figure 6.b Illustrates the diffractograms of the fraction <2 µm (untreated, glycolated under ethylene glycol, and heated to 500°C), sampled (BPT 1) representative collected in the study area. The bulk mineralogical composition of Trebia bentonite is much diversified it should be noted that all bentonites have their main peaks successively assigned mainly montmorillonite (M) (4.43 to 29.07%), feldspar-K (Fd-K) (19.29 to 34.93%), hematite (Hm) (4.18 to 18.97%), anorthite (An) (5.65 to 17.23%), cristobalite (Cr) (4.93 to 63.96%), and secondary minerals with a content of less than 10%, quartz (Qz) (0.54 to 2. 62%), anatase (At) (0.2 to 1.7%). A moderate amount of calcite (Ca), (1.05 to 4.67%), dolomite (D) (1.14 to 4.25%), pyrite (py) (0.59 to 2.34%), and with traces of rhodochrosite (Rdh), zeolite (ZL) and xenotime (Xn).

In the Trebia deposit, bulk mineralogy is characterized by the association of two types of montmorillonites. The first diffraction peaks (001) of montmorillonite occur at a basal spacing of 15Å and 12 Å. Theoretically, the peak at 15Å (d001) corresponds to a calcium pole (M-Ca) present in all samples and the peak at 12 Å (d_{001}) corresponds to a sodium pole (M-Na). The other three peaks are located at 4.48 Å (d_{110}), 2.16Å (d_{200}) and 1.49 (d_{060}). The d_{060} reflection at 1.49 Å indicates the dioctahedral character of smectite (Inglethorpe et al. 1993; Kumpulainen and Kiviranta 2010). During the transition from perlite to rhyolite, we notice the disappearance of hematite and the appearance of pyrite, as well as the disappearance o f x enotime and the appearance of zeolite. The clay fraction (<2µm) consists mainly of smectite ,illite, kaolinite, chlorite and chlorite and regular mixed layer composed of illite/smectite and smectite/chlorite. Smectite is the main component of the clay fraction (> 90%) of all samples were identified at normal slide (LN) at d001 reflection 12 Å, at 16Å under ethylene glycol solvation (LEG) and at 9 Å after slide dehydration heated to 500 C° ($LH_{500C°}$).

The peak at a d-spacing of 5Å at reflection d002 corresponds to Illite, identified in all samples does not exceed 3% of the clay fraction. Kaolinite has been identified with normal blade and ethylene glycol at 7Å (d001), after heating to 500 °C is destroyed. The clay fraction gradually varies from contact with perlite to contact with rhyolite, including decrease in smectite content, disappearance of kaolinite and appearance of chlorite at a basal spacing of 4.47Å (d003), as well as appearance of other types of interlayer ordered two-component (illite / smectite) to (smectite / chlorite).

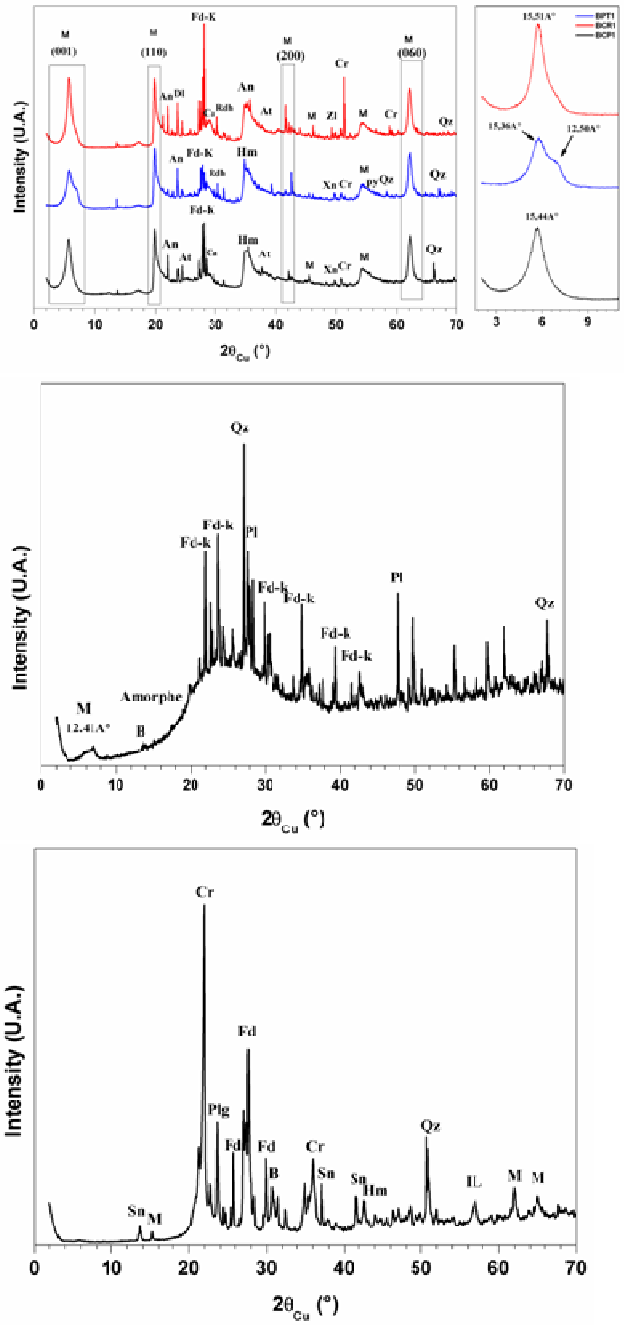

Fig. 6.a Bulk mineral composition of the studied samples

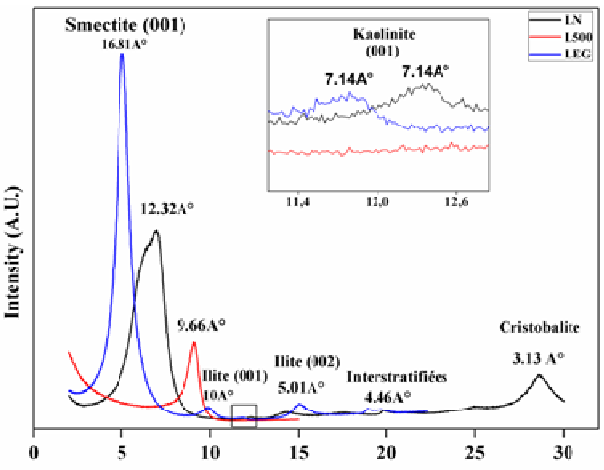

Fig. 6. b. Clay mineral composition of BPT_1 sample

Perlite of Trebia (PT) is essentially composed of feldspar-K (53.09%) plagioclase (29.5%), and quartz (14.09%), the amorphous part being silicate glass. The peak at a spacing of 12. 41 Å at d001 reflection corresponds to montmorillonite (3.25%). The clay fraction (<2 µm) consists mainly of smectite (97.82%) and illite (2.17%). Rhyolite (RHT) with a very diversified mineralogical composition is composed mainly of cristobalite (67.73%) and feldspar-K (18.63%) and secondary minerals with a content of less than 10%, plagioclase (6.73%), montmorillonite (2.14%), hematite (1.88%), quartz (1.37%), sanidine (0.73%), illimenite (0.5%) and biotite (0.27%). With the clay fraction (<2 µm) formed of smectite (52.93%), chlorite (33.37%), illite (8.73%) and kaolinite (4.96%).

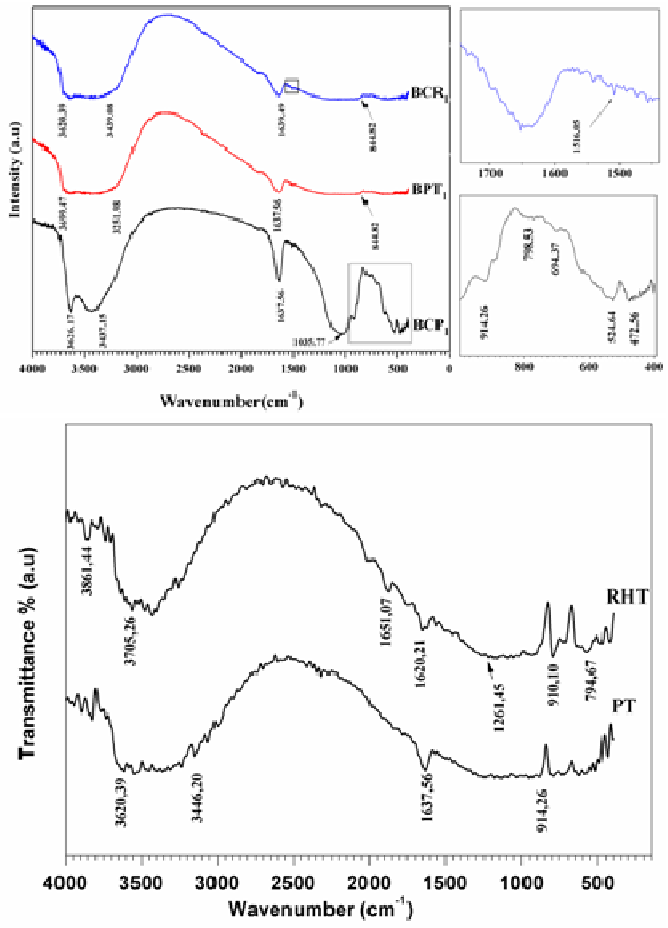

Fig. 7. Infrared spectra of the analyzed profiles and limit areas

FTIR characterization

Fig. 7 shows the FTIR analyses were performed in the 400-4000 cm^{-1} range of samples of bentonite, perlite and Trebia rhyolite. The presence of clay phase absorption bands and crystalline impurities. All profiles are characterized by a very high absorption in the region greater than 3629.17, 3620.39, 3699.47, 3629.17, 3699.47, 3699.47, 3695.61, 3624.25, 3643.53, 3705.26 cm^{-1} and region less than 1035.77, 1637.56, 1035.77, 914.26 844.82 cm^{-1}. The profile type 1 (PT_1) characterized by a very strong multiple absorption band observed from 3626.17 to 3431.15 cm^{-1} (BCP_1), from 3699.47 to 3251.98 cm^{-1} (BPT_1) and from 3620.39 to 3439.08 cm^{-1} (BCR_1), are assigned the OH hydroxyl elongation of the structure octahedral layer coordinated either to the aluminum atom or with two aluminum atoms.

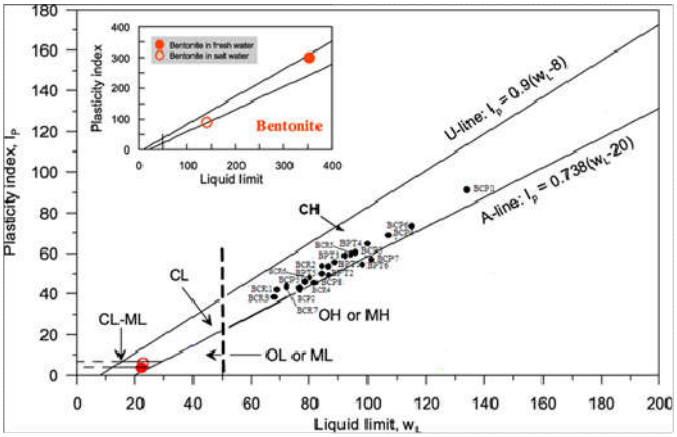

Fig.8 Position of bentonite samples on the plasticity maps for the classification of fine-grained soils

In the case of this profile, the peak 3627. 17 cm^{-1}(BCP_1) reveals the presence of aluminum, and the peak appears more around 3699.47 cm^{-1} (BPT_1) and thus reveals the presence of magnesium in the structure of the bentonites analyzed (Mehdi2014; Nay ak and Singh 2007; Brahimi et al. 2015; Serir 2015), are indicative of the presence of two types of smectite showing OH stretching bands on the inner surface at 3629.17 and 3620.39 cm^{-1} for montmorillonite and 3699.47 cm^{-1} for beidellite (Kumpulainen and Kiviranta 2010). Followed by a large band at 3437.15, 3251.98 and 3439.08 cm^{-1} in the mineral is attributed to OH stretching (ν_3) structural hydroxyl groups and wat er p resent in the mineral. This indicates the possibility of the hydroxyl bond between the octahedral and t etrahedral layers(R avindra Reddy et al. 2017).

The profiles 4 and 6 characterized by the appearance of specific peaks corresponding to the deformation vibrations of the bonds of water molecules appears from 2374.37 to 2627.97 cm-$_1$ (PT_4), and from 2347. 37 to 2380.16 cm^{-1} (PT_6). The band at 2380 cm^{-1} was assigned to carbonates or bicarbonat es and did not change with the pilosity (Balci and Gokcay 2009). However, a very strong and intense band observed at 1645.56 cm^{-1} (BCP_1, BPT_1) and 1639.49 cm-1 (BCR_1) is due to ν2 the asymmetric OH stretching, in other words the OH deformation of the water adsorbed between the layers and the OH elongation constitution (Hajjaji et al. 2002; Khatem 2017). The band at 1516.05 cm^{-1} (BCP_1) is attributed to the mode of d eformation the interlayer water of clay (Kumpulainen and Kivirant a 2010). The vibration observed at 1035.77 cm-^{1} (BCP^1) shows that the Si-O elongation, the band corresponding to the Al-Al-OH deformation, are observed at 914.26 cm^{-1} (Zaitan et al. 2008), indicate the possibility of hematite (Nayak and Singh 2007). The presence of band at 844.82 cm^{-1} in all samples bandes is attributed to Al-Mg-OH deformations (Mehdi 2014; Hajjajiet al. 2002). For BCP_1 characterized by, the vibration observed at 798.53 cm-1 corresponding to Si-O, Si-O-Al, (Al, Mg) -O-H (Nayak and Singh 2007). The band at 694.37 cm^{-1} is assigned to Si-O and Si-O-Al, indicate the possibility of the cal cite (Nayak and Singh, 2007), Also the deformation of Al-O-Si, Si-O-Mg and Si-O-Si of clayey minerals occurred at 536.64 and 472.56 cm^{-1}, respectively (Hajjaji et al. 2002; Mehdi 2014; Nayak and Singh 2007). In this way, all attributed bands of (Si-O-Si) and (Si-O) showing the presence of silicate minerals such as quartz or cristobalite. All low bands that have occurred in the range 924 cm^{-1} (BPT_1), and 550 cm^{-1} (BCR_1) must result from octahedral and/or tetrahedral substitutions (Hajjaji et al. 2002).

Table 3. Representative mineralogical analyses for the studied samples

	Sample		BCP1		BPT1		BCR1		PT		RHT	
			d(Å)	Weight (%)	d(Å)	Weight (%)	d(Å)	Weight (%)	d(Å)	Weight (%)	d(Å)	Weight (%)
Bulk mineralogy	M*		15	27,17	15	25,41	15	23,91	12,41	3,25	1,49	2,14
	Cr*		1,79	8,42	1,79	8,34	1,78				4,04	67,73
	Fd-K*		3,21	28,51	3,21	19,88	3,19	27,38	3,77	53,09	3,22	18,63
	An*		4,03	9,06	3,75	9,54	2,54	11,51	-	-		
	Hm*		2,52	18,97	2,53	18,32	-	-	-	-	2,11	1,88
	At		2,37	1,58	2,37	1,11	2,37	0,91	-	-	-	-
	C		3,04	2,99	3,12	4,36	3,12	3,39	-	-	-	-
	Xn		1,82	0,58	1,83	0,82	-	-	-	-	-	
	Qz		1,41	1,54	2,45	2,62	4,18	2,11	3,29	14,09	1,79	1,37
	Dlm		2,84	1,14	4,05	2,9	4,04	3,69	-	-	-	-
	py		-	-	1,63	2,34	1,6	0,59	-	-	-	-
	Rdh		-	-	2,84	4,31	2,84	2,3	-	-	-	-
	Zl		-	-	-	-	1,62	0,45	-	-	-	-
	Plg		-	-	-	-	-	-	3,21	29,5	3,76	6,73
	B		-	-	-	-	-	-	10,03	0,046	2,93	0,27
	IL		-	-	-	-	-	-	-	-	1,62	0,5
	Sn		-	-	-	-	-	-	-	-	2,16	0,73
Clay mineralogy	Smectite	LN	12,51	97,03	12,32	97,62	12,41	91,76	15,1	97,82	14,8	52,93
		LEG	16,81		16,81		15,01		16,89		16,63	
		LH500°C	9,68		9,66		9,66		9,99		10,01	
	Kaolinite	LN	7,14	0,29	7,14	0,17		-	-	-	7,16	4,96
		LEG	7,14		7,14				-		7,16	
		LH500°C	-		-				-		-	
	ilite	LN	5	1,66	5	1,6	5	0,71	10	2,17	9,87	8,73
		LEG	5		5		5		10		9,87	
		LH500°C	-		-		5		-		-	
	chlorite	LN	-	-	-	-	3,52	7,4	-	-	3,53	33,37
		LEG	-		-		3,52		-		3,53	
		LH500°C	-		-				-		-	
	mixed layer	LN	4,46	1,12	4,47	0,48	4,85	0,128	-	-	-	-
		LEG	4,46		4,47		4,85		-		-	
		LH500°C	-		-		-		-		-	

This slight shift towards the low frequen cies would be due to the presence in tet rahedral sites of t rivalent ions (Al^{3+}) substituted with silicon and ferric ions in octahedral sites (Brahimi et al. 2015), thus indicate the possibility of presence of hematite (Nayak and Singh 2007). The examination the FTIR spectra of perlite showed broad range of wav e numbers observed at 3620.39 cm^{-1} followed by a broad band at 3446.20 cm^{-1} in the mineral, Covering at the same time in the stretching OH (ν_3) of stru ctural hydroxyl groups and water present in perlite as well as the spectral region typical of free water (Kaufhold et al. 2014; Ravindra Reddy et al. 2017). This indicates the possibility of the hydroxyl bond between the o ctahedral and t etrahedral layers (Kumpulainen and Kiviranta 2010), in two atoms of aluminum (3620 cm^{-1}) and one atom of aluminum and one atom of magnesium (3446.20 cm^{-1}) (Mehdi 2014), so reveals the presence of magnesium in the structure of perlite. The very strong and intense band observed at 1637.56 cm^{-1} is attributed to ν_2 asymmetric OH stretching of water and is a structural part in the mineral (Balci and Gokcay 2009). The peaks in 2901 and 2988 cm^{-1} correspond to the vibrations of deformation the connections of the water molecules (Mehdi 2014). The spectre presents an intense absorption band between 914.26 and 1261.45 cm^{-1}; it characterizes the elongation vibrations of the Si-O bond. The vibration bands appear in the interval 439.77-550 cm^{-1} signals the metals Al, Mg, and Fe located in octahedral position (Bouras 2003). The low bands in 779.24, 785.03, and 630.37 cm^{-1} typical of impurities are manifested by shoulders that we attribute to the presence of quartz (Bouras 2003). The rhyolite characterized by a set of bands that occurred in the region 3700-3800 cm^{-1} are assigned to Al-OH-Al (Ravindra Reddyet al. 2017), with an intense peak and shoulders in 3664.75 and 3402.36 cm^{-1}, corresponds to the elongation vibrations of the OH groups (ν_3) and the possibility of a hydroxyl bond between the octahedral and tetrahedral layers (Ravindra Reddy et al. 2017). This indicates the presence of montmorillonite (Bouras 2003). A very intense band observed at the interval 1651.07-1620.21 cm^{-1} due to ν_2 stretching H-O-H to the water molecules adsorbed between the sheets (Cariat et al. 1981; Gupta et al. 2013). The recorded spectrum of the rhyolite shows an intense absorption band between 910.10 and 1261.45cm^{-1}, characterizes the elongation vibrations of the Si-O bond. We note the presence o f a weak peak of vibration at 1398.39 cm^{-1}due to calcite ($CaCO_3$) (Bouras 2003). The characteristic bands of impurities appear in 794.67- 719.45 cm^{-1}, are assigned to quartz band (Gupta et al. 2013).

Chemical analysis: The bentonite samples (Table 3) are characterized by a large amount of Fe between 12.2 and48.9 % related to iron ore such as hematite (Fe_2O_3), identified by both XRD analysis and FTIR spectra, the Si content from 0.1to 16.7%, is related to quartz, cristobalite and feldspar,with respect to the amount of Al (5.5 to 12%), Ca (from 9.65to 18.3%) between slips play the role of compensating ions of charge deficit, and Mg (from 26.3 to 31.1) is attributed to Montmorillonite - (Na, Ca) 0.3 (Al, Mg) $2Si_4O_{10}(OH)_2(H_2O)$, identified by XRD analysis and FTIR spectra. On the other hand Mg present except at BPT_1 and BCR_4 this explains the aluminum of the octahedral layer is partially replaced by magnesium (Zaitan et al. 2008), and also assigned to the presence of dolomite, identified in the FTIR spectra. Quantities of K (3.3 to 16.3 %), aluminium (Al) are attributed to alkaline feldspar, clay minerals, and also to mica.

The lowest amount of P (from 2. 7 to 4. 5 %) and Y (from 0.02 to 0.06%) assigned to the presence of Xenotime (YPO_4), this mineral forms as a consequence of local mobilization and process concentration during the metamorphic recrystallization of the clay fraction, without the need to involve external source (Cabella et al. 2001) , so this explains the presence of Th and U (Bastos Neto et al. 2012) identified by the XRD analysis, S (from 1.2to 2. 3%), indicate the presence of pyrite (FeS_2) This is in agreement with the furnished in formation by analysis DRX. Mn (from 0.6 to 1.6 %) assigned to the presence of rhodochrosite ($MnCO_3$). Very low levels of Ti (from 0. 7 to 2. 6%) indicate the presence of Antase.

Table 4. Chemical composition of bentonite, perlite and rhyolite samples from Jbel Tdiniet

	BCP1	BCP4	BCP6	BPT1	BPT4	BPT6	BCR1	BCR4	BCR6	PT	RHT
Mg	-	-	-	29.3	-	-	-	26.3	-	29.1	31.1
Fe	40.2	42.3	37.6	28.6	48.9	41.1	42.1	37.5	35.2	18.5	12.2
K	6.4	5.6	5.4	4.4	5.06	5.7	5.8	3.3	13.1	15.2	16.3
Ca	17.1	18.3	16.7	11.1	15.1	17.0	15.8	9.6	17.4	12.6	14.0
Si	16.7	15.02	16.7	0.1	13.4	14.8	15.7	9.8	14.8	11.1	12.4
Al	9.7	9.5	12.0	7.3	8.7	11.0	10.3	5.5	11.3	6.5	6.1
P	4.3	4.0	4.5	3.1	3.8	4.1	4.1	2.7	4.1	2.8	3.3
S	2.2	2.1	2.3	1.6	1.8	1.9	1.9	1.3	1.9	1.2	1.5
Ti	1.6	1.5	1.6	1.2	1.3	2.6	1.5	1.3	0.7	1.0	1.2
Mn	-	-	1.6	0.8	0.3	-	1.1	1.4	-	0.6	1.0
Rb	0.07	0.07	0.06	0.05	0.06	0.05	0.06	0.04	0.1	0.4	0.3
Sr	0.5	0.6	0.5	0.4	0.5	0.6	0.5	0.4	0.5	0.2	0.2
Zr	0.6	0.5	0.6	0.3	0.5	0.6	0.5	0.3	0.5	0.2	0.2
Th	0.2	0.2	0.2	0.1	0.2	0.2	0.2	0.1	0.1	0.08	0.1
Zn	0.08	0.07	0.05	0.08	0.1	0.1	0.09	0.2	0.08	0.03	-
Y	0.05	0.05	0.06	0.02	0.05	0.04	0.03	0.03	0.04	0.03	0.02
As	0.02	0.02	-	0.02	0.02	-	-	0.01	-	0.02	0.02
Pb	-	-	0.04	-	-	-	-	-	-	-	-
Sn	-	-	-	0.07	-	-	-	-	-	-	-
U	-	-	-	-	-	-	-	-	-	0.01	0.02
Mo											0.01
Cu	-	-	-	-	-	-	-	-	-	-	0.02

Atterberg limits: The limits of Atterberg are an indicator of the property of connection of a bentonite (Inglethorpe et al. 1993). From the water contents that delimit the four states of consistency are called consistency limits or Atterberg limits that include the plastic limit (PL), the liquid limit (LL) and the plastic index (PI), are plotted on the plasticity map proposed by Casagrande in 1932 (Fig. 8). The map shows that all the bentonites of Trebia are characterized by high plasticity, with the BCP_1 being very plastic relative or otherwise. Generally there are various factors affecting the properties of plasticity such as the origin of the geological formation, the mineral composition, the particle size distribution, the impurities (non-clay minerals) and the organic matter (Daoudi et al. 2014), so the silt faction is the BCP_1 sample gives them great plasticity. According to the literature, bentonites are characterized by very high liquidity limits compared to other clay minerals, so the liquid limit test can be a sensitive indicator of the response of a Ca- bentonite or Na-b entonite exchange. In general, Ca- bentonites give LL values between 100 and 200 and Na-bentonite values can be up to 750 (Inglethorpe et al. 1993; Zeng et al. 2019). The very high liquidity limits for all samples vary between 74 and 137, so from the LL values two types can be deduced, Ca-bentonite and Na-bentonite.

Conclusion: Chemical analysis, XRF, XRD and FTIR show that Trebia- Jbel Tdiniet bentonites are diversified, the mineralogical composition consists of a mixture o f a variable proportion of clay, hematite, anorthite, and cristobalite, quartz, anatase, calcite, dolomite, xenotime, pyrite, rhodochrosite and zeolite in small quantities, the presence of the above minerals was confirmed by an FTIR analysis. The X-ray fluorescence (XRF) study shows that bentonites are mainly composed of alumina and silica in large quantities and iron oxide and others in small quantities. Petrographic studies show that Trebia bentonites probably result from hydrothermal alterations from perlite to bentonite. On the other hand and after the results obtained in this preliminary characterization tudy lead us to consider future research, focused on the experimentation of these raw materials on a semi-industrial scale to evaluate in particular their us e the bentonite such as absorbents, and the perlite used for insulation.

Acknowledgment: The financial support is provided by the CNRST "Projets dans les domaines prioritaires de la recherche scientifique et du développement technologique" (Re f. PPR1/2015/63). We would like to thank Professor Nathalie Fagel and Dr. Meriam El Ouahabi, University of Liège (Geology, UR Clays, Geochemistry and Sedimentary Environments (AGEs)) for the XRD analysis of various samples.

REFERENCES

Abdelouas A 1996. Étude de l'altération de verres rhyolitiques au contact de saumures naturelles (Bolivie)- Application à l'étude du comportement à long terme du verre nucléaire R7T 7.Thèse Doctorat d'Etat, Université Louis Pasteur, Strasbourg 1.

Ait Hmeid H, Akodad M, Aalaoul M, Baghour M, Moumen A, Skalli A, Daoudi L 2019. Particle size distribution and statistic analysis of the g rain size messinian bentonite from the kert bassin (north ern Morocco). Materials Today: Proceedings 13:505–514.

Ait Hmeid H, Akodad M, Aalaoul M, Baghour M, Moumen A, Skalli A, Anjjar A, Conti P, Sfalanga A, Ryazi Khyabani F, Minucci S, Daoudi L 2020. Clay mineralogy, chemical and geotechnical characterization of bentonite from Beni Bou Ifrour Massif(the Eastern Rif , Morocco). The Geological Society of London 502. https://doi.org/10.1144/SP502-2019-25

ASTMD 3418 1983. Standard Test Methods for Liquid Limit, Plastic Limit, and Plasticity Index of Soils. Book of ASTM Standards 4(8):1-16.

Azdimousa A, Jabaloy A, Asebryi L, Booth-Rea G, Bourgois J, Rezqui H, Aït Brahim L 2011. Circuit C9 : Rif oriental, in A. Michard, O. Saddiqi, A. Chalouan and A MouttaqiNouveaux Guides géologiques et miniers du Maroc. Notes et Mém. Serv.Géol. Maroc 5(560):91- 122.

Balci S, Gokcay E 2009. Pore structure and surface acidity evaluation of Fe-PILCs. Turkish Journal of Chemistry 33:843–856.

Bastos Neto AC, PEREIRA VP, Pires AC, Barbanson L, Chauvet A 2012. Fluorine-rich xenotime from the world-class madeira Nb–Ta–Sn deposit associated with the albite-enriched granite at pitinga, Amazonia, Brazil. The Canadian Mineralogist 50:1453-1466.

Bouras O 2003. Proprietes adsorbantes d'argiles pontees organophiles: synthese et caracterisation. Thèse de doctorat de l'université de Limoges Faculté des Sciences et Techniques Ecole Doctorale Sciences Technologie et Santé.

Brahimi S, Boudjema S, Rekkab I, Choukchou-Braham A, Bachir R 2015. Synthesis and Catalytic Activity of Vanadia-Doped Iron-Pillared Clays for Cyclohexene Epoxidation.Research Journal of Pharmaceutical, Biological and Chemical Sciences 63: 63-76.

Cabella R, Lucchetti G, Marescotti P 2001. Authigenic monazite and xenotime from pelitic metacherts in pumpellyite–actinolite-facies conditions, sestri–voltaggio zone, central Liguria, Italy. The Canadian Mineralogist. 39:717-727.

Cariati F, Erre L,Micera G,Piu P, Gessa C 1981. Water molecules and hydroxyl groups in montmorillonites as studied by near in frared sp ectroscopy.Clays and Clay Minerals. 29:157-159.

Christidis GE, Scott PW, Marcopoulos T 1995. Origin of the bentonite deposits of eastern milos, aegean, greece: geological,

mineralogical and geochemical evidence. Clays and Clay Minerals. 43:63–77.

CookHE, Johnson PD, Matti JC, Zemmels I 1975. Methods of sample preparation and X-ray diffraction data analysis, X-ray mineralogy laboratory. In: Hay es, Eds. Initial Report DSDP 28. U.S. Govt. Printing Office, Washington, 999–1007.

Daoudi L, Elboudour Elidrissi H, Saadi L, Albizane A, Bennazha J, Waqif M, Elouahabi M, Fagel N 2014. Characteristics and ceramic p roperties of clayey materials from Amezmiz region Western High Atlas, Morocco. Applied Clay Science 102:139–147. https://doi.org/10. 1016/j. clay.2014.09. 029.

Ddani M, Meunier A, Zahraoui M, Beaufo rt D, EL Wartiti M, Fontaine C, Boukili B, El mahi B 2005. Clay mineralogy and chemical composition of bentonites from the gourougou volcanic massif northeast morocco. Clays and Clay Minerals 533. :250–267.

El Bakkali S, Gourgaud A,Bourdier JL, Bellon H, Gundogdu N 1998. Post-collision neogene volcanism of the Eastern Ri f Morocco: Magmatic evolution through time. Lithos 45:523–543.

Folk RL, Ward WC 1957. Brazos River bar: a study in the significance of grain size parameters. Journal of Sedimentary Petrology 27:3-26.

Frey R, Yovanovich B, BurghelleJ 1936. Composition and probable genesis of some decolorizing clays of North Africa. Serv. Min. and Carte Geol, Morocco: 38-65.

Grim R E, Guven N 1978. Bentonites: Geology, Mineralogy, Properties and Uses. Developments in Sedimentology 24:229-232.

Gupta A, Amitabh V, Kumari B, Mishra B 2013. FTIR and XRPD Studies for the Mineralogic al Composition of Jharkhand. Research Journal of Pharmaceutical, Biological and Chemical Sciences 43: 360–369.

Hajjaji M, Kacim S, Boulmane M 2002. Mineralogy and firing characteristics of a clay from the valley of Ourika Morocco. Applied Clay Science 213/4: 203–212. https://doi.org/10. 1016/S0169-131701. 00101-6.

Hernandez J 1983. L evolcanisme Miocène du Ri f Oriental Maroc: Géologie, pétrologie et minéralogie d'une province shoshonitique. Thèse de doctorat de l'université Pierre et Marie Curie, Paris VI, France, pp 592.

Hernandez J, Bellon H 1985. K-Ar radiometric chronology of Miocene volcanics in eastern Morocco: tectonic and magmatologic. Revue de Geologie Dynamique et de Geographi e Physique 262 :85-94.

Hyun S P, Cho YH, Hahn PS, Kim SJ 2001. Sorption mechanism of UV on a reference montmorillonite : Binding to the internal and external sur faces. Journal of Radio analytical and Nuclear Chemistry 250:55–62.

Inglethorpe SDJ,Morgan DJ, Highley DE, Bloodworth A 1993. British Geological Survey: Industrial Minerals Laboratory Manu al. Journal of Mathematics pp 124.

Kau fhold S, Reese A, Schwiebacher W, Dohrmann R, Grathoff GH, Warr LN, Halisch M, Müller C, Schwarz-Schampera U, Ufer K 2014. Porosity and distribution of water in perlite from the island of Milos , Greece. SpringerPlus ed. 3598. :1-10.

Kelessidis V C, T samantaki C, Dalamarinis P 2007. Effect of pH and electrolyte on the rheology of aqueous Wyoming bentonite dispersions. Applied Clay Science 38:86–96.

Khatem R 2017. Etude des propriétés adsorbantes des argiles modifiées vis à vis de polluants organiques: Cas des pesticides Et des produits pharmaceutiques. Thèse de doctorat de l'université Abdel hamid ibn badis, Mostaganem, pp. 175. http://hdl.handle. net/123456 789/557.

Knechtel MM, Patterson SH 1962. Bentonite deposits of the northern Black Hills District Wyoming, Montana and South Dakota. US Geol Surv Bull 1023:893-1029

Kouloughli S 2007. Etude experimentale des melanges sable bentonite leurs Perfo rmances comme Barrières de Confinement dans les CET. Thèse de doctorat de l'université Mentouri, Constantine.

Kumpulainen S, and Kiviranta L 2010. Mineralogical and Chemical Characterization of Various Bentonite and Smectite-Rich Clay Materials: Part B: Mineralogical and Chemical Characterization of Clay Materials. Posiva working report 52:37-41.

Louaya A, Hamoumi N 2010. Etude morphostructurale de la région de Nador Maroc nord-oriental. Africa Geoscience Review 172 :107–127.

Maychou S 2009. Étude morphostructurale et cartographie SIG du Rharb Septentrional et du Prérif Maroc. . Analyse sismotectonique et modélisation de la déformation de la région demoulay Bousselham. Thèse de doctorat de l'université Chouaïb doukkali, El Jadida.

McManus J, 1988. Grain size distribution and interpretation. In: Tucker, M.E. Ed., Techniques in Sedimentology. Blackwell, Oxford, pp 63–85.

Mehdi F 2014. Modification de la bentonite par un sel de diphosphonim applications à l' adsorption des colorants textiles rouge, bleu et jaune Bemacide. . Mémoire du master de l'université Abou bekr belkaid, Tlemcen.

Millogo Y 2008. Etude géotechnique, chimique et minéralogique de matières premières argileuse et latéritique du Burkina Faso améliorées aux liants hydrauliques : application au génie civil bâtiment et route. . Thèse de doctorat de l'université Ouagadougou.

Moore DM, Reynolds RC 1989. X-Ray Diffraction and the Identi fication and Analysis of Clay Clay Minerals. Oxford University P ress, Oxford , pp 332.

Nayak P S, Singh BK 2007. Instrumental characterization of clay by XRF, XRD and FTIR. Bulletin of Materials Science 303. :235–238.

Odom I E 1984. Smectite clay minerals: properties and uses. Phil. Trans. R. SOC. Lond. A3ll, pp 391-409.

Qlihaa A, Dhimni S, Melrhaka F, Hajjaji N, Srhiri A 2016. Physico-chemical characterization of a morrocan clay. Journal Mater Environ 75:1741-1750.

Ravindra Reddy T, Kan eko S, Endo T, Lakshmi Reddy S 2017. Spectroscopic Characterization of Bentonite. Journal of Lasers, Optics & Photonics 43. :1-4.

Rollet P, Bouaziz R 1972. L'analyse thermique- les changements de phase. Tome1. Gautier- Villards Ed. , pp 250.

Ross J S 1963. Bentonite in Canada. Dept. Mines & T echn. Surv, Ottawa, Monograph, pp 873.

Rotella M, Simandl G 1996. Marilla perlite - volcanic glass occurrence , british Columbia, Canada. Industrial Minerals with emphasis on Western North America, pp 263–272.

Sadran G, Millot G, Bonifas M 1955. The origin of bentonite deposits at Lalla Maghnia Oran. . Serv. Carte Geol., Algeria, Bull 5:213-234.

Serir S 2015. Préparation et caractérisation des VOx et NiOx supportéssur la Bentonite inte rcalée au fer. Application à l' époxydation ducyclohexène. Thèse de doctorat de l'université de Tlemcen.

Termier H, Termier G, Korenko V 1956. On the occurrence of bentonite of Miocene age between Menerville and Dra-el-Mizane, Algeria. Serv. Carte Geol., Algeria 8:291-301.

Underwood MB, Basu N, Steurer J, Udas S 2003. X-RAY diffraction a nalysis , with application to DSDP site 297 Shikoku basin. Proceedings of the Ocean Drilling Program 190196. :1-28.

Vista R L 1992. Clays. Annual Report 1990, US Bureau of Mines.

Zaitan H, Bianchia D, Achakb O,Chafi T 2008. A comparative study of the adsorption and desorption of o-xylene onto bentonite clay and alumina. Journal of Hazardous Materials 153:852–859.

Zeng Z, Cui Y J, Zhang F, Conil, N, Talandier J 2019. Investigation of swelling pressure of bentonite/claystone mixture in the full range of bentonite fraction. Applied Clay Science 178:1-7. https://doi.org/10.1016/j.clay.2019.105137.

****